Journal of Interfaces, Thin films, and Low dimensional systems 2 (2017-2018) 57-64

Synthesis and characterization of nHA-PLA composite coating on stainless steel 316L by dip-coating process for biomedical applications

S. Mohammadzadeh Asl[1], M. Ganjali[1*], M. Alizadeh[2], M. Shahlaei[1], A. Sohrabi Jam[1]

[1] *Bioengineering Group, Nanotechnology and Advanced Materials, Materials and Energy Research Center, (MERC), Tehran, P.O. Box 14155-4777, I. R. Iran*

[2] *Department of Materials Engineering, Isfahan University of Technology, Isfahan, P.O. Box 84156-83111, I. R. Iran*

ARTICLE INFO

Article history:
Received 23 January 2018
Revised 3 March 2018
Accepted 23 April 2018
Available online 1 May 2018

Keywords:
Nano hydroxyapatite
Poly lactic acid
Stainless steel
Dip coating

ABSTRACT

316L stainless steel is the most commonly used metallic material in the manufacture of orthopedic implants. To achieve better properties metal implants are often coated with biocomposites. A sol–gel method was used for coating Poly lactic acid (PLA)/Hydroxyapatite nanopowder (nHA) on stainless steel 316L substrate. 10g PLA was added to 100 gr chloroform and stirred for 2 h at 60 °C. Then 0.5g nHA was added and continued to stir for 30 min at 60 °C to form a jelly-like solution. Afterwards, the substrate was immersed into the solution and kept for 2, 5, and 15 minutes and withdrawn from the bath solution at a prescribed withdrawal velocity. The X-ray diffraction (XRD) and Fourier transform infrared spectroscopy (FTIR) were utilized in order to evaluate the phase composition and the functional groups of PLA/nHA coatings. Morphology and thickness of the nanocomposites coating of samples were evaluated using scanning electron microscope (SEM). Cell viability asses and eventually corrosion resistance were evaluated by MTT and potentiostat test, respectively. SEM result shows that the deposition rate is measured (in terms of coating thickness) as a function of immersion/soaking time. The results of XRD and FTIR tests confirmed the presence of phase of PLA/nHA nanocomposites in the coated samples. Furthermore, the corrosion resistance of coated samples was increased with immersion or soaking time in the solution bath of PLA/nHA nanocomposites and was higher than the uncoated sample.

1 Introduction

The stainless steel 316L is one of the most popular metallic biomaterials that has good ability to bear significant loads and undergo plastic deformation prior to failure, as indicated by their respective ultimate tensile strength (UTS) and fracture toughness. It is used in temporary devices such as internal fixation or traction devices due sufficiently corrosion resistant for long-term as an implant material. In these applications, the devices are removed after healing has taken place. Therefore, it is important to develop methods to increase the performance and the service life of these materials by changing the material's surface composition, the structure, and the morphology, which leave intact the mechanical properties of these metallic biomaterials.

Coating method is the most popular way to protect metal biomaterials. There are quite a few kinds of coatings methods, such as plasma or thermal spraying [1], sol-gel [2], laser cladding [3] have been widely

*Corresponding author.
Email address: Monireh_ganan@Merc.ac.ir
DOI: 10.22051/JITF.2018.19010.1021

used for this purpose and have received commercial success over other alternatives. Currently, some surface modifications such as ceramic polymer composite coating similar with the hard tissues of the body consisting mainly of inorganic apatite crystals and organic collagen fibers and carbonated apatite have been studied. Nanosized hydroxyapatite (nHA) is the main component of mineral bone. HA have excellent biocompatibility and bioactivity properties with respect to bone cells and tissues, probably because of its similarity with the hard tissues of the body.

Despite many advantages, apatites produced in the bulk form possess a low mechanical strength when used as a single constituent for load-bearing sites. Therefore, various bioceramic-polymer composites for bone-grafting material were prepared and relationship between material structure and properties has been studied [4, 5]. Among synthetic polymers used in bone tissue engineering such as Polymethyl methacrylate (PMMA) [6], polylactide (PLA) [7], polyglycolide (PGA) [8], polyvinyl alcohol (PVA) [9] and polyethylene glycol (PEG) [10], the polylactic acid (PLA) is probably the most widely investigated biodegradable and bioresorbable polyester [11].

Polylactic acid or polylactide (PLA) is a thermoplastic and biodegradable aliphatic polyester derived from naturally occurring organic acid (lactic acid). PLA is inexpensive, dimensionally stable and harder than Polytertafluoroethylene (PTFE). It melts at a lower temperature (in the range of 180-220°C) with glass transition temperature 60-65°C. Furthermore, PLA and its composites are biodegradable in nature; they degrade easily in physiological conditions as shown in animal model by simple hydrolysis of the ester backbone resulting in the formation of non -harmful and non-toxic compounds. Their degradation products are easily eliminated in the form of carbon dioxide and water from the kidneys. PLA can also be recycled to its monomer by thermal depolymerization or hydrolysis. It can be processed by injection molding, extrusion, spinning film and casting, providing easy access to a wide range of materials. High molecular weight polylactides are absorbed completely and their rate of absorption depends on molecular weight, morphology, and enantiomeric purity of the polylactides.

The sol–gel method has recently received more attention than other coating methods because it can be processed and formed easily without demanding high temperatures. The materials based on polylactic acid (PLA) and hydroxyapatite (HA) have been suggested as promising solutions for implant coating in order to improve reconstruction of bone defects, to reduce risk of inflammation and implant rejection. Shaovalova et al. [12] reported the bioresorbable composites using biocompatible poly-L-lactide (PLA) with HA and evaluated its effect on bone remodeling rate. This study shows that the PLA/HA bone-like layer on surface of coatings enhance ossification in the bone reconstruction process. In another study, Ahmet Çakir and et al. [13] used PVA to improve adhesion properties of HA coating on Ti–6Al–4V. They demonstrate the effect of time deposition on the thickness of coatings.

2 Materials and methods

a. Synthesis of HA nanopowder (nHA)

HA nanopowder was prepared according to Safronova et.al. One liter of a 1 M water solution of calcium chloride was added by drops to 1 liter of a 0.6 M water solution of potassium hydrophosphate containing KOH. The reaction was conducted at 60°C with constant mixing. Synthesis was conducted at pH=8–9. The pH level was maintained by adding a two-fold KOH excess relative to the amount calculated from the equation of the reaction. The precipitate obtained was allowed to sit in the mother liquor for 30 min. Then, the precipitate was separated from the mother liquor and washed with distilled water 3 times in order to remove KCl in the precipitation material and dried in a thin layer over a period of 48 h. Finally, the samples were calcined at a temperature interval up to 700°C with a heating rate of 10°C/min. The final temperature was kept for 1 h [14].

b. Preperation of PLA/nHA composites coating on 316L substrate

At first, for suspension preparation, 10 gr Polylactic acid (PLA; Aldrich) dissolved in 100 ml chloroform (CCl4 Aldrich; extra pure) is heated at 60 °C and stirred at 400 rpm for 2 hours till a jelly-like material is formed. Then 5wt% of nHA gradually added to solution and continues heating and stirring for 30

minutes. It is then that the suspension is ready for the dip coating process. The elements in the stainless steel sheet are assessed by the quantimeter experiment (Table 1). Steel sheet samples prepared in dimensions of 3×1×1 cm^2 and polished, finally dip coated in suspension for 2, 5, 10 minutes. Note that all the chemicals used in this research are purchased from Merck Company and the chemical compositions of the stain steel 316L elaborated for this study after quantmetry analyze is shown in table 1 [15].

Table 1- Chemical composition of stainless steel 316L according to ASTM standard along with chemical elements of samples used.

	Fe %	**C % max**	**Si % max.**	**Mn % max.**	**P% max.**
316L	Balance	.02	0.589	1.1	0.081
316L standard	Balance	.03.	.75	2	.045
	S % max.	**Cr %**	**Mo%**	**Ni %**	**Cu % max**
316L	0.0416	16.68	2.18	11.7	0.406
316L standard	0.3	16-18	2-3%	10-14	1

Crystalline phase and crystallite size of prepared powder and coatings were carried out by XRD (Philips PW 3710, Cu Kα, 30 KV, 35 mA) experiment. Morphology and size of the nanocomposites and surface and cross section of coating samples were evaluated using scanning electron microscope (SEM) (VEGA, TESCAN) equipped EDX. Functional groups of nHA powder were determined by Fourier transform infrared spectroscopy (FTIR) (VEGA, TESCAN). MTT assay was used to test the cell viability. A cell on day 1 was used for the assay. 50 µL MTT (KeyGEN, Nanjing, China) was added per well and incubated at 37°C for 2 h. The media were carefully removed and 200 µL DMSO (Gibco, USA) was added into each well. The absorbances were measured at 490 nm using a microplate reader (BioTek, Winooski, USA). Polarization potentiodynamic test was performed by (Autolab, Model µIII, Echo-Chemi) in SBF. SBF solution was prepared regarding to Kocobo [16]. Briefly, the following procedure was done:

1. Wash all the bottles and wares with 1N-HCl solution, neutral detergent, and ion - exchanged and distilled water, and then dry them.
2. Put 500 ml of ion-exchanged and distilled water into one litter polyethylene bottle, and cover the bottle with a watch glass.
3. Stir the water in the bottle with a magnetic stirrer, and dissolve the reagents one by one in the order as given in Table 2 (One after the former reagent was completely dissolved).
4. Adjust the temperature of the solution in the bottle at 36.5°C with a water bath, and adjust pH of the solution at pH 7.40 by stirring the solution and titrating 1N-HCl solution (When the pH electrode is removed from the solution, add the water used for washing the electrode to the solution).
5. Transfer the solution from the polyethylene bottle to a volumetric glass flask. Add the water used for washing the polyethylene bottle to the solution in the flask.
6. Adjust the total volume of the solution to one litter by adding ion-exchanged and distilled water and shaking the flask at 20°C.
7. Transfer the solution from the flask to a polyethylene or polystyrene bottle, and store the bottle in a refrigerator at 5-10°C (If some substance is precipitated in the solution during the storage, do not use this solution as SBF and its container again).

Table 2: reagent used in SBF preparation.

Order	Reagent	Amount
1	NaCl	7.996 gr
2	$NaHCO_3$	0.350 gr
3	KCl	0.224 gr
4	$K_2HPO_4.3H_2O$	0.228 gr
5	$MgCl_2.6H2O$	0.305 gr
6	1M-HCl	40 ml
(About 90% of total amount of HCL to be added)		
7	$CaCl_2$	0.278 gr
8	Na_2SO_4	0.071 gr
9	$(CH_2OH)_3CNH_2$	6.057 gr

c. Corrosion test

For investigating the behavior of corrosion, the experimental conditions were determined by equilibrium between opposing electrochemical reactions. One reaction is the anodic reaction, in which a metal is oxidized, releasing electrons into the metal. The other is the cathodic reaction, in which a solution species (often O_2 or H^+) is reduced, removing electrons from the metal. When these two reactions are in equilibrium, the flow of electrons from each reaction is balanced, and no net electron flow (electrical current) occurs. The two reactions can take place on one metal or on two dissimilar metals (or metal sites) that are electrically connected.

The Tafel corrosion method offers the following significant advantages:

1. Under ideal conditions the accuracy of the Tafel extrapolation method is equal or greater than conventional weight loss methods.
2. With this technique it is possible to measure extremely low corrosion rates, and it can be used for continues monitoring the corrosion rate of a system.
3. Tafel Plots can provide a direct measure of the corrosion current, which can be related to corrosion rate.
4. The rapid determination of corrosion rates with Tafel Plots can be advantageous for such studies as inhibitors evaluation and alloy comparisons.

d. MTT assay

The MTT assay is a simple nonradioactive colorimetric assay to measure cell cytotoxicity, proliferation, or viability. MTT is a yellow, water-soluble tetrazolium salt. Metabolically active cells are able to convert this dye into a water-insoluble dark blue formazan by reductive cleavage of the tetrazolium ring. Formazan crystals, then, can be dissolved in an organic solvent such as dimethylsulphoxide (DMSO) and quantified by measuring the absorbance of the solution at 550 nm, and the resultant value is related to the number of living cells. To determine cell cytotoxicity/viability, the cells were plated at a density of 1×10 cells/well in a 96-well plate at 37 ºC in 5% CO_2 atmosphere. After 24 h of culture, the medium in the wells was replaced with the fresh medium containing nanoparticles in varying concentrations. After 24 h, 20 µl of MTT dye solution (5 mg/ml in phosphate buffer pH 7.4, MTT Sigma, Dorset, U.K.) was added to each well. After 4 h of incubation at 37 °C and 5% CO_2 for exponentially growing cells and 15 min for steady-state confluent cells, the medium was removed and formazan crystals were solubilized with 200 µl of DMSO and the solution was vigorously mixed to dissolve the reacted dye. The absorbance of each well was read on a microplate reader (Dynatech MR7000 instruments) at 550 nm. The spectrophotometer was calibrated to zero absorbance, using culture medium without cells. The relative cell viability (%) related to control wells containing cell culture medium without nanoparticles was calculated by [A]test/[control] ×100.

3 Results and discussion

3.1 nHA powder

3.1.1 *Phase characterization*

XRD analysis of synthesized nHA shown in Fig. 1. The hydroxyapatite peaks characterized in this image with sign o. As seen there is KCl peak in pattern that it's because of synthesis process. Estimation of size of synthesis crystals done with this pattern and scherrer equation. According to Scherer equation (Eq. 1) D is the mean size of the ordered (crystalline) domains (A°), λ is the X-ray wavelength (A°), θ is the Bragg angle (in degrees) and B is the line broadening at half the maximum intensity (FWHM), after subtracting the instrumental line broadening, in radians. With this equation mean size of crystalline were about 23nm.

$$D = \frac{0.9\lambda}{B\cos\theta} \quad (1)$$

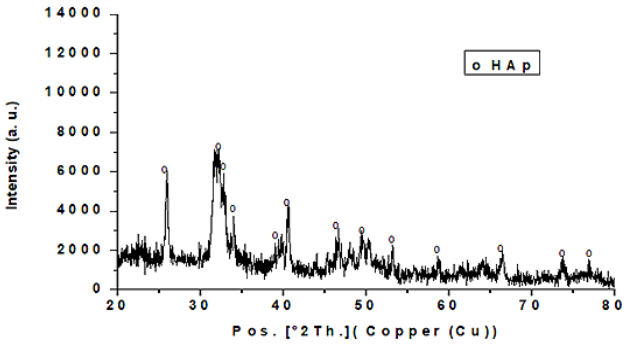

Fig. **1**: XRD pattern of nHA powder.

3.1.2 *Microstructure and morphology*

SEM of synthesized powder is shown in the Fig. 2. As seen in this image morphology of crystallite are spherical and at nanometer size. Mean size of crystallite measured by ImageJ and was 25nm.

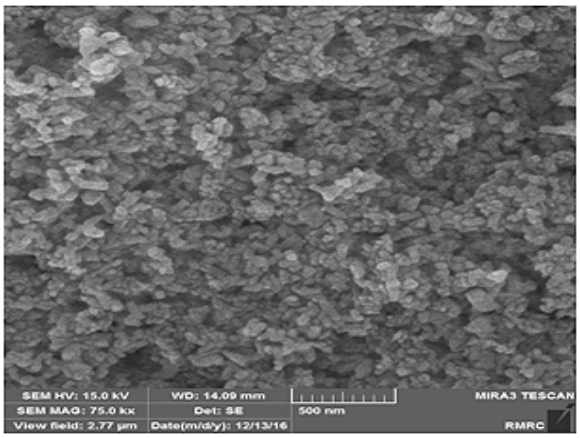

Fig. 2: morphology of nHA powder.

3.2 PLA/nHA composites

3.2.1 *Fourier transform infrared (FTIR) spectroscopy*

It can be seen that all the peaks at 2949-2997; 1749; 1182, 1127,1082, 1044 cm-1 assigned to –CH-; -C=O Carbonyl; -O-C-O; -C-O- in –CH-O- and –C-O- in –O-C-O was observed for PLA respectively. Also, the peak at 3200–3700 cm-1 observed for the ion stretching vibration around 3568 cm-1 confirms the presence of a hydroxyl groupi. Likewise, the FTIR spectrum analysis is compared with the result of Wu et al.ii for the confirmation and exhibited that –Ca=O stretching vibration peaks were formed at 1750–1760 cm-1. The results revealed that branched and cross-linked macromolecules may be produced in PLA/HA because the copolymer has carboxyl groups to react with the hydroxyl groups of HA.

3.2.2 *Phase characterization of PLA/nHA composite coatings*

Figure 2 a-c depicts the XRD spectra of PLA/nHA composite coatings at various time depositions of 2, 5 and 10 minutes. As can be seen in Fig. 3, in all samples, HA and PLA characteristic peaks appear around 2θ = 25-55° and 16-29° respectively [19]. Furthermore, because the HA nanopowder used in the solution is 5wt%, the corresponding peaks become very small.

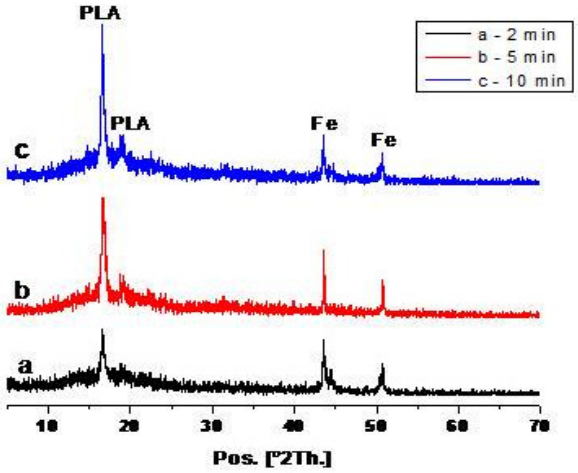

Fig. 3: XRD patterns of PLA/nHA composite coatings at various time depositions a) 2, b) 5 and c) 10 minutes.

3.2.3 *Microstructure of PLA/nHA composite coating*

Figs.4a–c show cross section of the PLA/nHA composite coatings at various time depositions. As seen in Fig. 4a-c, the mean thicknesses of coatings at various time depositions is equal to 2, 5, and 10 minutes with 1.24, 3.46 and 4.87 µm, respectively. From this figure it can also be noticed that the thickness of PLA/nHA composite coatings increases with the deposition time.

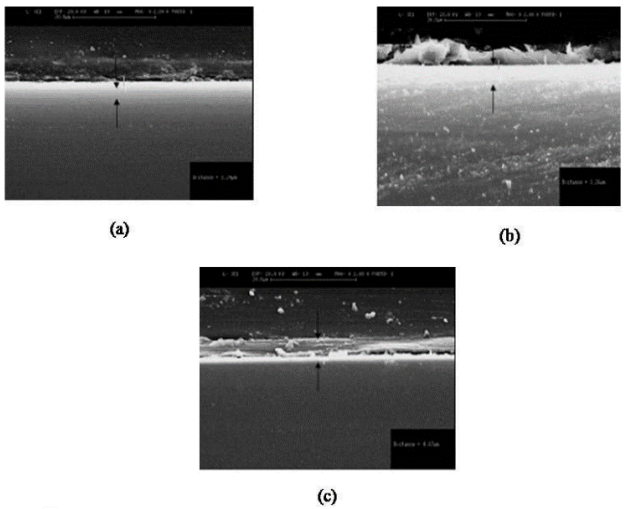

Fig. 4: SEM images for dip coated times from top to bottom 2, 5 and 10 minutes.

It is possible to observe that the coatings have dense and uniform coating structure with absence of delamination and/or cracks at the interface. The attained results are in good agreement with those reported by Liu and et. al [20], where thin film hydroxyapatite deposits onto sandblasted 316L stainless steel substrates prepared using water-based sol–gel technique. They explained the formation of the coatings that were dense and firmly attached.

3.2.4 *MTT Assay and Microscopy Observation of PLA/nHA composite coatings*

Cells used in this test were fibroblast and cell toxicity assased for 1 day in culture medium. Fig. 5a-d shows optical microscopy (OM) image for a) positive control, and samples that are dip coated for b) 2, c) 5 and d) 10 minutes. It can be seen that cells disperse everywhere and spread on the surface. The cells are not spindle like which is indication of biocompatibility of samples. Individual nucleus seen in the image correspond to cells that have died shown by points. Cell viability of dip coated samples for 2, 5, and 10 minutes were respectively, 73.34%, 77% and, 71.6% that are acceptable.

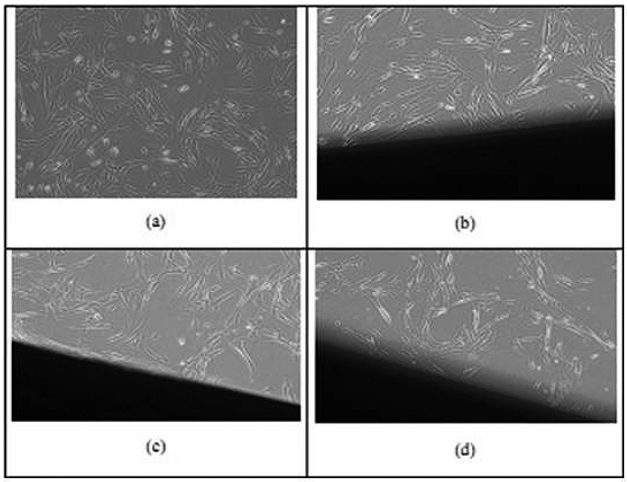

Fig. 5a-d. Optical microscopy (OM) image for a) positive control, and samples that dip coated for b) 2, c) 5 and d) 10 minutes.

3.2.5 *Corrosion test*

The blue curve in Fig. 6 is related to stainless steel without coating immersed in SBF for 4 days. $I_{corrosion}$ is intersection of the two branches which gives $I_{corrosion}$ = -5.1. The orange curve in this figure corresponds to stainless steel that coated for 2 min before immersed in SBF for 4 days. For this curve we have $I_{corrosion=}$ -4.9. The yellow curve also corresponds to stainless steel which is dip coated for 5 min and immersed in SBF for 4 days. For this we have $I_{corrosion}$= -5.2. The grey curve corresponds to stainless steel which is dip coated for 10 min before immersed in SBF solution for 4 days. For this we have $I_{corrosion}$=-5.6. It is known that if $I_{corrosion}$ decends, the corrosion rate reduces, this the corrosion resistance increases. The other parameter for comparing the corrosion resistance which is of importance is $E_{corrosion}$ which is specified by the Y axis. It could be noticed that when $E_{corrosion}$ increases, the corrosion rate decrease. This the corrosion resistance increases. It could be readily seen in Fig. 6, $E_{corrosion}$ of stainless steel without coating immersed in SBF for 4 days, stainless steel that is coated for 2 min before being immersed in SBF for 4 days, stainless steel which is dip coated for 5 min before being immersed in SBF for 4 days, and stainless steel that is dip coated for 10 min before being immersed in SBF solution for 4 days are respectively, -0.18, -0.05, -0.11, -0.09. It is obvious that $E_{corrosion}$ of dip coated samples are higher than without coating sample. This, the corrosion resistance of dip coated samples are higher. In one work Sol-gel thin coatings of ZrO_2, SiO_2, $70SiO_2$-$30TiO_2$ and $88SiO_2$-$12A1_2O_3$ compositions (mole %) have been prepared from sonocatalyzed sols and deposited by the dip-coating technique on 316L stainless steel foils. The influence of the coatings on the chemical corrosion of the substrate has been measured through potentiodynamic polarization curves in aqueous 15% H_2SO_4 solution between 25 and 50°C. The values of the corrosion potential, polarization resistance and corrosion rate have been determined.

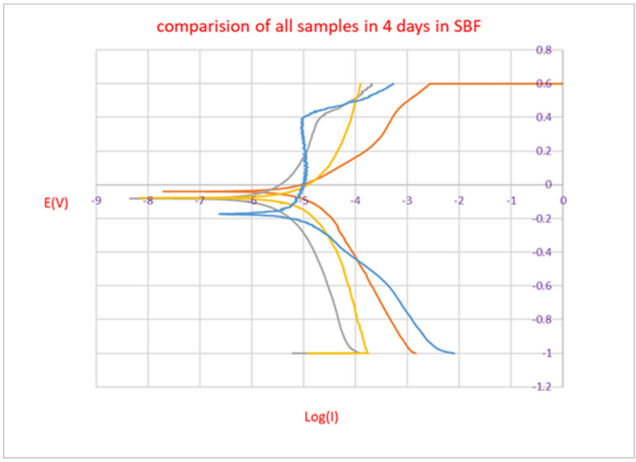

Fig. 6: Potentiodynamic polarization curves for different samples.

Analysis of the data combined with scanning electron microscopy studies indicate that the films act as a geometric blocking against exposure to the corrosive media and increase the lifetime of the substrate up to a factor 8.5. By comparison it can be seen that $I_{corrosion}$ of coated samples with nHA-PLA are lower than coated samples with ZrO_2, SiO_2, $70SiO_2$-$30TiO_2$. So nHA-PLA coated samples are more resistant to corrosion.

4 Conclusions

nHA-PLA composite coating on the substrate of stainless steel 316L was successfully formed by dip coating process. Coating thickness was about 5 micrometer and homogeneity of that was good for use in biomedical applications. The sol-gel method used was easy to process and need ambient temperature. Cell toxicity of samples which were low had acceptable cell viability being more than 70% after 1 day placing in the culture medium. The corrosion rate of samples decreased after the coating process.

References

[1] Steve Weiner, and H. Daniel Wagner. "The material bone: structure-mechanical function relations." Annual Review of Materials Science, **28** (1998) 271.

[2] Matsumura, Kazuaki, Takashi Hayami, Suong Hyu Hyon, and Sadami Tsutsumi. "Control of proliferation and differentiation of osteoblasts on apatite□coated poly (vinyl alcohol) hydrogel as an artificial articular cartilage material." Journal of Biomedical Materials Research Part A, **92** (2010) 1225.

[3] Hong Li, Wu Yang, Ge Yunsheng, Jia Jiang, Kai Gao, Pengyun Zhang, Lingxiang Wu, and Shiyi Chen. "Composite coating of 58S bioglass and hydroxyapatite on a poly (ethylene terepthalate) artificial ligament graft for the graft osseointegration in a bone tunnel." Applied Surface Science, **257** (2011) 9371.

[4] Tao Liu, Xinbo Ding, Dongzhi Lai, Yongwei Chen, Ridong Zhang, Jianyong Chen, Xinxing Feng et al. "Enhancing in vitro bioactivity and in vivo osteogenesis of organic–inorganic nanofibrous biocomposites with novel bioceramics." Journal of Materials Chemistry B, **2** (2014) 6293.

[5] R. Govindan, G. Suresh Kumar, and E. K. Girija. "Polymer coated phosphate glass/hydroxyapatite composite scaffolds for bone tissue engineering applications." RSC Advances, **5** (2015) 60188.

[6] F. S. Senatov, K. V. Niaza, M. Yu Zadorozhnyy, A. V. Maksimkin, S. D. Kaloshkin, and Y. Z. Estrin. "Mechanical properties and shape memory effect of 3D-printed PLA-based porous scaffolds." J. of the mechanical behavior of biomedical materials, **57** (2016) 139.

[7] K. De Groot, R. Geesink, C. P. A. T. Klein, and P. Serekian. "Plasma sprayed coatings of hydroxylapatite." J. Biomedical Materials Research Part A, **21** (1987) 1375.

[8] LinShu Liu, Young Jun Won, Peter H. Cooke, David R. Coffin, Marshal L. Fishman, Kevin B. Hicks, and Peter X. Ma. "Pectin/poly (lactide-co-glycolide) composite matrices for biomedical applications." Biomaterials, **25** (2004) 3201.

[9] S. Mollazadeh, J. Javadpour, and A. Khavandi. "In situ synthesis and characterization of nano-size hydroxyapatite in poly (vinyl alcohol) matrix." Ceramics International, **33** (2007) 1579.

[10] J. Milton Harris, *Poly (ethylene glycol) chemistry: biotechnical and biomedical applications.* Springer Science & Business Media, 2013.

[11] S. Saha and S. Pal. "Mechanical properties of bone cement: a review." J. Biomedical Materials Research Part A, **18** (1984) 435.

[12] Yelena G. Shapovalova, Lyudmila A. Rasskazova, A. Gudima, Vyacheslav V. Ryabov, Anatoliy G. Filimoshkin, Irina A. Kurzina, Julia Kzhyshkowska, and Darya N. Lytkina. "Bioresorbable composites based on hydroxyapatite dispersed in poly-L-lactide matrix." European J. of cancer supplements, **13** (2015) 49.

[13] Ahmet Çakir, Funda Ak Azem, and Güler Ungan. "Use of polyvinyl alcohol to improve adhesion properties of hap coating on Ti–6Al–4V." J. Biomechanics, **44** (2011) 21.

[14] M. P. Ferraz, F. J. Monteiro, and C. M. Manuel. "Hydroxyapatite nanoparticles: a review of preparation

methodologies." J. Applied Biomaterials and Biomechanics, **2** (2004) 74.

[15] Bora Mavis and A. Cüneyt Taş. "Dip coating of calcium hydroxyapatite on Ti□6Al□4V substrates." J. of the American Ceramic Society, **83** (2000) 989.

[16] Tadashi Kokubo, *Bioceramics and their clinical applications*. Woodhead Publishing, 2008.

[17] Xiaofei Ma, Jiugao Yu, and Ning Wang. "Compatibility characterization of poly (lactic acid)/poly (propylene carbonate) blends." J. Polymer Science Part B: Polymer Physics, **44** (2006) 94.

[18] Chin San Wu, "Improving polylactide/starch biocomposites by grafting polylactide with acrylic acid–characterization and biodegradability assessment." Macromolecular Bioscience, **5** (2005) 352.

[19] Mahshid Kalani and Yunus Robiah, "Effect of supercritical fluid density on nanoencapsulated drug particle size using the supercritical antisolvent method." International J. of nanomedicine, **7** (2012) 2165.

[20] Dean-Mo Liu, Quanzu Yang, and Tom Troczynski. "Sol–gel hydroxyapatite coatings on stainless steel substrates." Biomaterials, **23** (2002) 691.